Available online at www.sciencedirect.com
SCIENCE DIRECT
Chemical Physics Letters 418 (2006) 40–45
CHEMICAL PHYSICS LETTERS
www.elsevier.com/locate/cplett

# Electronic structures and hydrogenation of a chiral single-wall (6,4) carbon nanotube: A density functional theory study

Guixiao Jia, Junqian Li*, Yongfan Zhang

*Department of Chemistry, Fuzhou University, Fuzhou, Fujian, 350002, China*
*State Key Laboratory of Structural Chemistry, Fujian Institute of Research on the Structure of Matter, The Chinese Academy of Sciences, Fuzhou, Fujian, 350002, China*

Received 10 August 2005; in final form 6 October 2005
Available online 10 November 2005

**Abstract**

The electronic structures and the hydrogenation of a chiral single-wall (6,4) carbon nanotube have been investigated by density functional theory. Our results indicate that, along the long vector of the tube, the HOMO and LUMO exhibit well-regulated arrangement of the bonding and anti-bonding structures. The adsorption of odd hydrogen atoms on the tube leads to obvious deformations of the tubular structure and the hydrogenation of the (6,4) tube can be well predicted by examining the topology of HOMO.


## 1. Introduction

Since the discovery of carbon nanotubes (CNT) in 1991 [1], these materials have attracted intensive interests due to their potential applications in the field of nanotechnology [2,3], such as molecular electronics, electron field emitters, quantum nanowires, catalyst supports, chemical sensors and sorbents for hydrogen storage. Comparing to the traditional metal hydrides, CNT has the advantages of light mass and large exposed surface, and therefore, it can be used to design a new storage material for hydrogen [4–7]. In connection with this important technological application, there have been many studies of the adsorption of hydrogen on CNTs, including both experimental and theoretical aspects [6–21]. Experimentally, due to the complicated constitutes of CNT and other reasons relative to the control of experimental conditions, the reproducibility of result is poor and the controversy exits regarding to the hydrogen storage capacities reported by different authors [7,8]. Therefore, theoretical investigations provide a very useful way to reveal the nature of the hydrogen absorption on CNTs. At present, the theoretical studies of hydrogen adsorption on CNT are focused on the storage capacity and the possible adsorption sites by using Monte Carlo simulations and empirical potential methods [22–24]. Bauschlicher [11] pointed out that, for a (10,0) zigzag tube, F, H atoms prefer to be bound along the tubular axis direction. On the other hand, for an armchair CNT, such as (10,10) tube, the experimental and theoretical works indicate that fluorine atoms tend to be added along the circumferential direction of tube. The reason of the above difference is yet not clear.

In this work, a chiral (6,4) tube is investigated. Since the chiral CNT is the main components in the production of carbon nanotube [25], furthermore, according to our knowledge, the adsorption of hydrogen atoms on a chiral CNT has not been reported by the first principles method.

## 2. Models and computational method

Fig. 1 presents a mapping of a graphite sheet, and a CNT can be formed when the sheet is wrapped along the vector $C_h$ that is defined as,

$$C_h = na_1 + ma_2,$$

* Corresponding author.
*E-mail address:* jqli@fzu.edu.cn (J. Li).

0009-2614/$ - see front matter © 2005 Elsevier B.V. All rights reserved.
doi:10.1016/j.cplett.2005.10.096

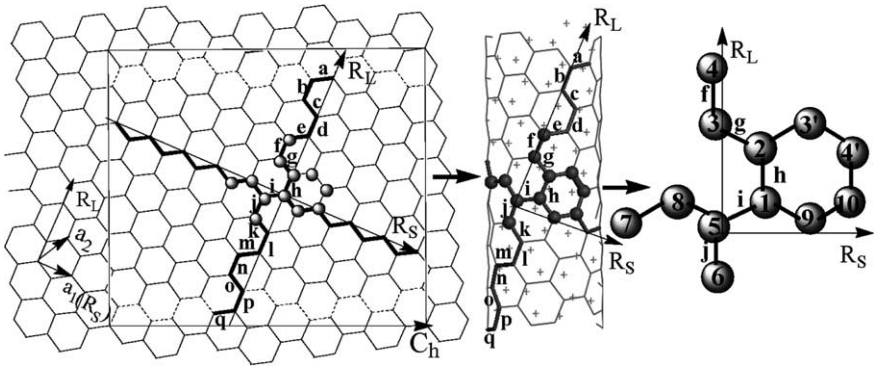


Fig. 1. Mapping of the graphene sheet to form the (6,4) CNT with a unit cell. The adsorption sites with the number are shown.

where $a_1$ and $a_2$ are the unit cell vectors, and $n$ and $m$ are integers. Besides the above vectors, two new vectors: one long vector $R_L$ and one short vector $R_S$, which are defined along $2a_2 - a_1$ and $a_1$ directions, respectively, are introduced in the present work. It is noted that when a graphite sheet is wrapped along $R_L$ vector, an armchair CNT is obtained, on the other hand, wrapping along $R_S$ vector results in a zigzag CNT.

In this work, a chiral (6,4) tube with finite length containing a unit cell is studied. Two models were considered, one is the tube with open ends (i.e., open-end (6,4) tube), containing 148 C atoms, and in another model the dangling bonds at the ends of the tube are saturated by hydrogen atoms (i.e., close-end (6,4) tube), containing 148 C and 20 H atoms. Some possible adsorption sites for H atoms are shown in Fig. 1 and are labeled by number to distinguish different adsorption models. For example, when one H is adsorbed on a carbon atom labeled as '1', we referred it to model '1'; when two H atoms are adsorbed on two C atoms labeled as '1' and '2', it is referred to model '1-2'. In addition, we also used letters from 'a' to 'q' to denote those C–C bonds along the $R_L$ vector. We will see that the topology of HOMO of (6,4) tube exhibits alternation of bonding and antibonding along the $R_L$ vector (see Fig. 2). However, along the $R_S$ vector, similar arrangement of C–C bonding is not observed. Hence, we focus on the adsorption sites along the $R_L$ and $R_S$ vectors, and to study the different hydrogenation behaviors between them.

In here, the adsorption energy ($E_a$) is calculated by the following formula,

$$\begin{aligned} E_a &= [E'_{\text{tube}-n\text{H}} - E_{\text{tube}} - nE_{\text{H}}]/n \\ &= [E'_{\text{tube}} + nE_{\text{H}} + nE_{\text{tube-H}} - E_{\text{tube}} - nE_{\text{H}}]/n \\ &= [E'_{\text{tube}} + nE_{\text{tube-H}} - E_{\text{tube}}]/n = E_d + E_{\text{tube-H}}, \end{aligned}$$

where $E'_{\text{tube}-n\text{H}} = E'_{\text{tube}} + nE_{\text{H}} + nE_{\text{tube-H}}$, represents the total energy of the adsorption system which contains n hydrogen atoms. $E_{\text{tube}}$ and $E'_{\text{tube}}$ are the energies of the tube before and after hydrogenation respectively. $E_{\text{H}}$ and $E_{\text{tube-H}}$ are the energy of hydrogen atom and interactive energy between the tube and one hydrogen atom, respectively. $E_d = [E'_{\text{tube}} - E_{\text{tube}}]/n$, is defined as the deformation energy.

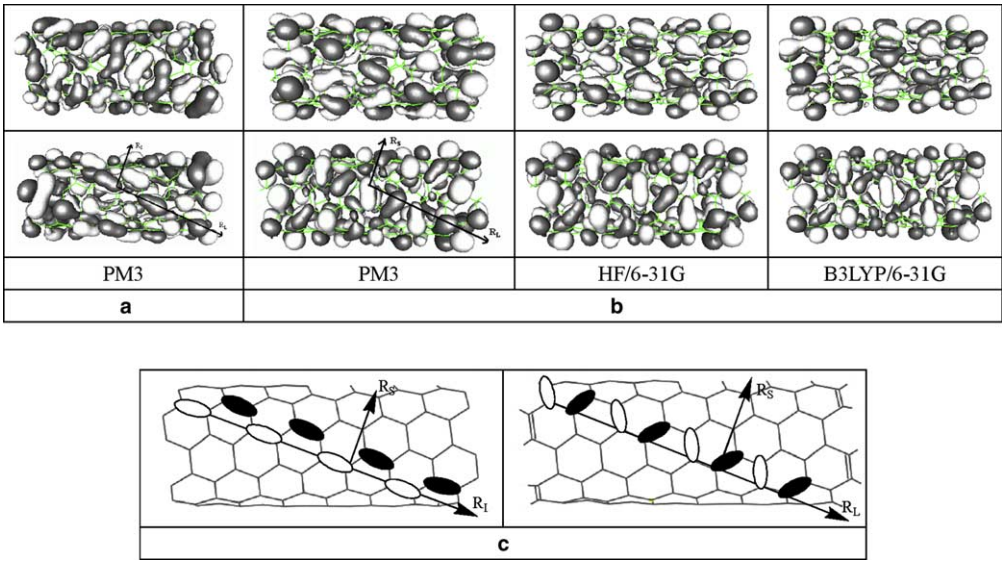


Fig. 2. (a) The LUMO (top) and HOMO (bottom) of the open-end (6,4) tube, and in HOMO the long and short vectors are signed. (b) The LUMO (top) and HOMO (bottom) of the hydrogen close-end (6,4) tube, and in HOMO the long and short vectors are signed. (c) The abbreviated frames of HOMOs for the open-end (6,4) tube (left) and the close-end (6,4) tube (right).

We have investigated the geometry and the electronic structure of close-end (6,4) tube at B3LYP/6-31G//PM3, B3LYP/6-31G//HF/6-31G and B3LYP/6-31G//B3LYP/6-31G levels, respectively. The results indicate that, the optimized structures and the topology of frontier orbitals are similar, and the system calculated in this work is consisted of 148 carbon atoms. So, to save computational time, the structural optimizations were carried out at PM3 level, and the adsorption energies and electronic structures were further determined at B3LYP/6-31G level. Furthermore, for some models, such as '1', '2', '1-2' and '1-5' adsorptions, the effects of basis set superposition errors (BSSE) were also considered. All calculations are performed by GAUSSIAN 03 package [26].

## 3. Results and discussion

### 3.1. Optimized structures of clean (6,4) tube

For the clean (6,4) tube, the optimized C–C bond lengths along $R_L$ vector are listed in Tables 1 and 2. For the open-end (6,4) tube optimized at PM3 level, except those C–C bonds at the both ends (such as bond a and q), the alternate arrangement of long and short C–C bonds along $R_L$ vector can be seen clearly. Table 2 lists the optimized C–C bond lengths for the close-end (6,4) tube calculated at PM3, HF/6-31G and B3LYP/6-31G levels. The results show that, the alternate structures of the long and short C–C bonds along the $R_L$ vector are similar with the open-end (6,4) tube. Moreover, from the data presented in Table 2, the lengths of the corresponding C–C bonds obtained by different methods are similar and the largest discrepancy is smaller than 0.03 Å. Therefore, to save computational time, in the following work, PM3 method is also employed to optimize the structures of H-adsorbed (6,4) tube. Actually, the rationality of PM3 method for the structural optimization of CNT has also been verified in several previous theoretical works [27–29].

### 3.2. The topology of frontier orbital of clean (6,4) tube

Fig. 2 displays the topologies of frontier orbitals of clean (6,4) tubes and the $R_L$ and $R_S$ vectors are also marked in the figure. In order to see the topologies of frontier orbitals clearly, the sketches of HOMOs along the long vector for the open-end and the close-end (6,4) tubes are given in Fig. 2c.

For the open-end (6,4) tube in Fig. 2a, the electronic structures obtained at B3LYP/6-31G //PM3 level indicate that, both HOMO and LUMO exhibit alternate arrangement of bonding and antibonding interaction along the $R_L$ direction. However, such alternate arrangement of bonding and antibonding is not observed along the $R_S$ vector. It is interesting to note that, the bonding and antibonding distribution of HOMO are consistent with the short and long distribution of C–C bonds.

For the close-end (6,4) tube, as shown in Fig. 2b, similar topologies of HOMO and LUMO are also found. The electronic structures of close-end tube calculated at B3LYP/6-31G//PM3, B3LYP/6-31G//HF/6-31G and B3LYP/6-31G//B3LYP/6-31G levels all exhibit the alternate arrangement of bonding and antibonding of C–C bonds along $R_L$ vector. Like the open-end (6,4) tube, the bonding interaction in HOMO is corresponding to the short C–C bond, while the antibonding interaction is corresponding

Table 1
The C–C bond lengths (Å) along the long vector for the open-end (6,4) tube obtained by PM3 method

| Label of C–C bond[a] | | Before adsorption | After adsorption | | | | | |
|---|---|---|---|---|---|---|---|---|
| Bonding[b] | Anti-bonding[b] | Clean | 2 | 1-2 (h)[c] | 1-5 (i) | 1-2-3 (gh) | 1-2-3-4 (fgh) | 1-2-3-4-5-6 (fghij) |
| | a | **1.424** | **1.385** | **1.428** | **1.417** | **1.393** | 1.436 | 1.436 |
| b | | **1.438** | 1.447 | **1.435** | **1.437** | 1.454 | **1.419** | **1.417** |
| | c | 1.440 | 1.435 | 1.446 | 1.447 | 1.489 | 1.459 | 1.460 |
| d | | **1.395** | 1.422 | **1.382** | **1.411** | 1.419 | **1.376** | **1.376** |
| | e | 1.439 | 1.430 | 1.446 | 1.429 | 1.425 | *1.507* | *1.508* |
| f | | **1.408** | 1.428 | **1.402** | **1.405** | *1.495* | *1.547* | *1.548* |
| | g | 1.445 | *1.503* | *1.509* | 1.427 | *1.550* | *1.552* | *1.551* |
| h | | **1.404** | *1.493* | *1.550* | *1.494* | *1.548* | *1.547* | *1.555* |
| | i | 1.439 | *1.482* | *1.511* | *1.576* | *1.505* | *1.508* | *1.554* |
| j | | **1.404** | 1.434 | **1.392** | *1.496* | 1.425 | **1.383** | *1.557* |
| | k | 1.445 | 1.408 | 1.458 | **1.406** | 1.438 | 1.462 | *1.507* |
| l | | **1.408** | *1.483* | **1.393** | 1.418 | 1.434 | **1.392** | **1.395** |
| | m | 1.439 | 1.423 | 1.446 | **1.414** | 1.424 | 1.448 | 1.449 |
| n | | **1.395** | 1.425 | **1.391** | 1.426 | 1.430 | **1.389** | **1.381** |
| | o | 1.440 | 1.420 | 1.445 | **1.420** | 1.433 | 1.446 | 1.449 |
| p | | **1.438** | 1.448 | **1.432** | 1.447 | 1.461 | **1.432** | **1.432** |
| | q | **1.424** | 1.447 | **1.427** | **1.396** | **1.385** | **1.427** | **1.428** |

The italic and boldface values show the C–C bond with long and short lengths, respectively.
[a] The bonds labeled along the long vector in Fig. 1.
[b] Corresponding to the bonding structures in HOMO of the open-end (6,4) tube.
[c] The letters in parenthesis show the bonds participated in hydrogenation.

Table 2
The C–C bond lengths (Å) along the long vector for the close-end (6,4) tube

| Label of bond[a] | | Before adsorption | | | After adsorption (PM3 level) | | | | |
|---|---|---|---|---|---|---|---|---|---|
| Bonding[b] | Anti-bonding[b] | Clean | | | 2 | 1-2 (h)[c] | 1-5 (i) | 1-2-3-4 (fgh) | 1-2-3-4-5-6 (fghij) |
| | | PM3 | HF | B3LYP | | | | | |
| a | | **1.381** | **1.376** | **1.400** | **1.407** | **1.368** | **1.385** | 1.419 | 1.417 |
| | b | 1.428 | 1.424 | 1.434 | 1.428 | 1.440 | 1.425 | **1.398** | **1.399** |
| c | | **1.403** | **1.398** | **1.424** | 1.429 | **1.407** | **1.404** | 1.434 | 1.433 |
| | d | 1.440 | 1.438 | 1.435 | 1.422 | 1.425 | 1.443 | **1.428** | **1.431** |
| e | | **1.399** | **1.394** | **1.424** | 1.428 | **1.394** | **1.402** | *1.507* | *1.508* |
| | f | 1.431 | 1.426 | 1.431 | 1.429 | 1.450 | 1.423 | *1.546* | *1.548* |
| g | | **1.407** | **1.401** | **1.429** | *1.504* | *1.504* | **1.398** | *1.548* | *1.547* |
| | h | 1.435 | 1.431 | 1.432 | *1.501* | *1.551* | *1.497* | *1.546* | *1.555* |
| i | | **1.400** | **1.396** | **1.425** | 1.416 | *1.511* | *1.574* | *1.508* | *1.554* |
| | j | 1.435 | 1.431 | 1.432 | 1.428 | 1.443 | *1.492* | **1.420** | *1.557* |
| k | | **1.407** | **1.401** | **1.429** | 1.432 | 1.421 | **1.398** | 1.444 | *1.504* |
| | l | 1.431 | 1.426 | 1.431 | 1.427 | **1.410** | 1.423 | **1.399** | **1.400** |
| m | | **1.399** | **1.394** | **1.424** | 1.427 | 1.418 | **1.402** | 1.437 | 1.452 |
| | n | 1.440 | 1.438 | 1.435 | 1.428 | 1.444 | 1.443 | 1.438 | **1.424** |
| o | | **1.403** | **1.398** | **1.424** | 1.427 | **1.410** | **1.404** | 1.422 | 1.432 |
| | p | 1.428 | 1.424 | 1.434 | 1.428 | 1.418 | 1.425 | **1.408** | **1.404** |
| q | | **1.381** | **1.376** | **1.400** | **1.407** | **1.394** | **1.385** | **1.409** | 1.420 |

The italic and boldface values show the C–C bond with long and short lengths, respectively.
[a] The bonds labeled along the long vector in Fig. 1.
[b] Corresponding to the bonding structure in HOMO of the close-end (6,4) tube.
[c] The letters in parenthesis show the bonds participated in hydrogenation.

to the long C–C bond. Similar results have also been observed for the armchair and zigzag tubes [29,30]. Therefore, it could be expected that the HOMO plays an important role to explain the properties of CNTs. In addition, except the fragment close to ending, the different treatments of the endings of CNT have small effects on the geometry and electronic structures of CNT.

### 3.3. Hydrogenation

#### 3.3.1. Rearrangement of C–C bonds

After hydrogenation, the C–C bonds around the adsorption site become single bonds and the bond lengths enlarge from 1.38–1.44 to 1.50–1.57 Å. Meanwhile, the transformation from $sp^2$ to $sp^3$ hybridization of the carbon atom leads to the outward deformation of the tube wall.

For the open-end (6,4) tube in Table 1, when odd hydrogen atoms are adsorbed, the alternate arrangement of the long and short C–C bonds along the $R_L$ vector is destroyed significantly, depicted by the deformation energies ($E_d$) (Fig. 3 and Table 3), resulting in endothermic adsorptions (Table 3). It is noted that, besides C–C bonds near the adsorption sites, the lengths of those C–C bonds far away from the adsorption sites also change obviously. For example, in Table 1 when one H atom is adsorbed on the C(2) atom, the length of the C–C bond labeled 'l' varies from 1.408 to 1.483 Å. Therefore, our results indicate that it is not adequate to only optimize a small fragment of the tube. When even hydrogen atoms are adsorbed, the alternate structure along the $R_L$ vector remains or is only rearranged, such as the models of '1-2' or '1-5' adsorption, which is corresponding to exothermic adsorption. Furthermore, according to the topology of HOMO for the open-end (6,4) tube, due to the bonding between C(1) and C(2) and the antibonding between the C(1) and C(5), compared with the '1-2' adsorption, the rearrangement of the alternate structure for '1-5' adsorption results in the small adsorption energy ($E_a$).

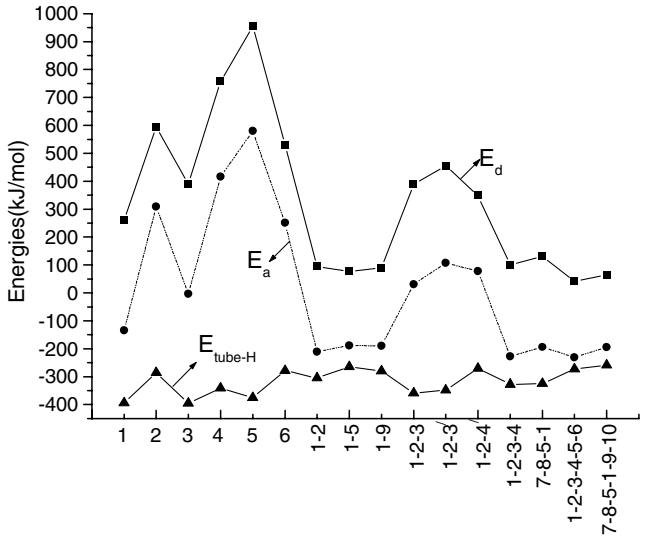


Fig. 3. $E_a$, $E_d$ for the open-end (6,4) tube and $E_{tube-H}$ between the open-end (6,4) tube and H atoms (kJ/mol).

For the close-end (6,4) tube in Table 2, when odd hydrogen atoms are adsorbed, the C–C bond lengths along the $R_L$ vector become average, which is different from the open-end (6,4) tube; for the adsorption of even hydrogen atoms, similar to the case of open-end tube, the alternate structure along the $R_L$ vector still remains or is only rearranged.

Table 3
The $E_a$ (kJ/mol), $E_d$ (kJ/mol), $E_{tube-H}$ (kJ/mol)

| Adsorbed site | open-end (6,4) tube | | | close-end (6,4) tube | | |
|---|---|---|---|---|---|---|
| | $E_a$ | $E_d$ | $E_{tube-H}$ | $E_a$ | $E_d$ | $E_{tube-H}$ |
| 1 | −133.76 | 260.49 | −394.25 | −127.15(−116.04)[a] | 39.59 | −166.74 |
| 2 | 308.84 | 594.15 | −285.31 | −101.59(−114.87)[a] | 77.83 | −179.42 |
| 3 | −3.80 | 390.94 | −394.74 | −94.14 | 42.19 | −136.33 |
| 4 | 416.41 | 757.40 | −340.99 | | | |
| 5 | 579.61 | 954.89 | −375.28 | | | |
| 6 | 250.96 | 529.17 | −278.21 | | | |
| 1-2 | −210.43 | 94.62 | −305.05 | −188.84(−180.64)[a] | 93.84 | −282.68 |
| 1-5 | −188.27 | 76.27 | −264.54 | −201.11(−193.46)[a] | 76.24 | −277.35 |
| 1-9 | −189.55 | 90.40 | −279.95 | | | |
| 1-2-3 | 31.04 | 389.62 | −358.58 | | | |
| 1-2-3′ | 107.00 | 455.26 | −348.26 | | | |
| 1-2-4′ | 78.06 | 348.14 | −270.08 | | | |
| 1-2-3-4 | −227.17 | 100.03 | −327.2 | −238.38 | 98.51 | −336.89 |
| 7-8-5-1 | −193.73 | 131.01 | −324.74 | −200.43 | 64.91 | −265.34 |
| 1-2-3-4-5-6 | −230.49 | 42.03 | −272.52 | −220.98 | 88.29 | −309.27 |
| 7-8-5-1-9-10 | −194.21 | 64.09 | −258.3 | −195.23 | 71.86 | −267.09 |

[a] $E_a$ through BSSE.

Comparing 1-2 model to 1-5 model, due to the rearrangement of the alternate structure, the smaller $E_a$ is obtained.

The calculated $E_a$ of each model is listed in Table 3, and for those models that the alternate structure of the bonding and antibonding remains or is only rearranged, the $E_a$ is exothermic , on the contrary, for the model that the alternate structure is destroyed, the corresponding $E_a$ is endothermic. Hence, it can be concluded that the alternate arrangement of bonding and antibonding of HOMO may be the inherent factor to affect the pattern of hydrogenation of the tube.

### 3.3.2. Energy analysis

The adsorption energies $E_a$ are calculated at B3LYP/6-31G//PM3 level. For the open-end (6,4) tube, when odd H atoms are adsorbed, except the 1 and 3 models, the hydrogenation of tube is endothermic and results in significant distortion of the tube wall. For the adsorptions of even H atoms , the hydrogenation is exothermic and the distortion of the tube is small (Fig. 3 and Table 3). Examining the absolute value of $E_a$, it shows the orders of 1-2 > 1-5 (or 1-9), 1-2-3-4 > 7-8-5-1 and 1-2-3-4-5-6 > 7-8-5-1-9-10, which implies that the adsorption of H atoms along the $R_L$ vector is favorable. The deformation energy $E_d$ of each model is also given in Table 3, and for comparison, the variations of $E_d$ and $E_a$ are presented in Fig. 3. As shown in this figure, the synchronous variation of $E_a$ and $E_d$ indicates that $E_a$ is strongly related with the deformation of the tube. The calculated value of $E_d$ is ranged from 40 to 955 kJ/mol and the obvious variation of the $E_d$ reflects good flexibility of the tubular structure in hydrogenation. Despite the endothermic adsorption of odd H atoms adsorbed on the open-end (6,4) tube, the interactive energies between the tube and adatoms, $E_{tube-H}$, are all exothermic, which shows adequately the deformation of the tube results in the endothermic adsorption.

In addition, for the open-end (6,4) tube, we also consider the adsorption of H atom at the both ends of tube. When two H atoms are adsorbed on each end in a way of $D_2$ symmetry, the average $E_a$ are −544.68 kJ/mol. For the adsorption of ten H atoms on each end, the close-end (6,4) tube is formed; in this case, the average $E_a$ is −456.03 kJ/mol. For comparison, the $E_a$ for the adsorption of four H atoms on the middle part of the open-end (6,4) tube is less than the half of that of adsorption on both ends. This reveals that the adsorption of hydrogen atoms on the ends of tube is most favorable.

For the close-end (6,4) tube, the rule of adsorption of even H atoms is similar to that of the open-end (6,4) tube. However, compared with the open-end tube, the absolute value of $E_a$ of 1-5 adsorption is larger than that of 1-2, due to the different topology of HOMO. As shown in Fig. 2c, there is a bonding between C(1) and C(5) atoms, and the antibonding between C(1) and C(2) atoms, which is opposite to the case of the open-end tube. Another difference is that, the adsorption of one H atom on the close-end tube is exothermic, while it is endothermic for the adsorption on the open-end tube. Therefore, the value of $E_a$ is sensitive to the treatment of the tube ends. We have known that the instable structure of the open-end (6,4) tube brings the tubular deformation, resulting in the endothermic adsorption. However, the hydrogen close-end (6,4) tube avoids it, and from Table 3, the deformation energies are smaller. For some adsorption models, namely, the models 1, 2, 1-2 and 1-5, the BSSE is also considered. Although the effect of BSSE on $E_a$ cannot be neglectable (about 10 kJ/mol), it does not change the relative order of $E_a$.

## 4. Conclusions

In this paper, the geometries, electronic structures and hydrogenation of the chiral (6,4) tube are investigated. For the clean tube, our results show the inherent relation

between the structure and the topology of HOMO, and both of them exhibit well-regulated arrangements along the $R_L$ vector. It is worth noting that, for the (6,4) tube, the adsorption of H atoms along the $R_L$ vector is preferable, and the bonding arrangement along the $R_L$ vector in HOMO can be adopted as an appropriate indicator to determine the pattern of hydrogenation of (6,4) tube. This important conclusion is also suitable to other types of CNT. As examples, for zigzag (10,0) and armchair (10,10) tube, the $R_L$ vectors are along the tube axis and circumferential directions, respectively, and they also show the alternate arrangement of the bonding and the antibonding along the $R_L$ vector [30,31]. Therefore, it could be expected that the H atoms tend to be adsorbed along the tube axis for (10,0) tube, while the sites at circumferential direction are preferable for (10,10) tube. These predictions are consistent with the results yielded by theoretical works [11,14].

The large change of the $E_d$ reflects obvious flexibility of the tubular structure in hydrogenation. Therefore, the optimizations of the structures before and after adsorptions are necessary. It is not adequate to only optimize a small part of the tube, specially, for the open-end (6,4) tube.

## Acknowledgements

The work is supported by the National Science Foundation of China (20273013, 20303002), the major NSFC of Fujian Province (2002 F010) and the State Key Laboratory of Structural Chemistry (020051).

## References

[1] S. Iijima, Nature 354 (1991) 56.
[2] S. Subramoney, Adv. Mater. 10 (1998) 1157.
[3] J. Kong, N.R. Franklin, C. Zhou, M.G. Chapline, S. Peng, K. Cho, H. Dai, Science 287 (2000) 622.
[4] L. Schlapbach, A. Züttel, Nature 414 (2001) 353.
[5] H. Rafii-Tabar, Phys. Rep. 390 (2004) 235.
[6] C. Liu, Y.Y. Fan, M. Liu, H.T. Cong, H.M. Cheng, M.S. Dresselhaus, Science 286 (1999) 1127.
[7] A. Chambers, C. Park, R.T.K. Baker, N.M. Rodriguez, J. Phys. Chem. B 102 (1998) 4253.
[8] A.C. Dillon, K.M. Jones, T.A. Bekkedahl, C.H. Kiang, D.S. Bethune, M.J. Heben, Nature 386 (1997) 377.
[9] R.T. Yang, Carbon 38 (2000) 623.
[10] Y. Ye, C.C. Ahn, C. Witham, B. Fultz, J. Liu, A.G. Rinzler, D. Colbert, K.A. Smith, R.E. Smalley, Appl. Phys. Lett. 74 (1999) 2307.
[11] C.W. Bauschlicher, Chem. Phys. Lett. 322 (2000) 237.
[12] C.W. Bauschlicher, Nano. Lett. 1 (2001) 223.
[13] C.W. Bauschlicher, R.S. Christopher, Nano. Lett. 2 (2002) 337.
[14] K.F. Kelly, I.W. Chiang, E.T. Mickelson, R.H. Hauge, J.L. Margrave, X. Wang, G.E. Scuseria, C. Radloff, N.J. Halas, Chem. Phys. Lett. 313 (1999) 445.
[15] M.X. Zhang, Y.F. Zhang, Y. Li, J.Q. Li, Chin. J. Struct. Chem. 22 (2003) 447.
[16] B.P. Tarasov, J.P. Maehlen, M.V. Lototsky, V.E. Muradyan, V.A. Yartys, J. Alloy Compd. 356–357 (2003) 510.
[17] K. Shen, T. Pietrass, J. Phys. Chem. B 108 (2004) 9937.
[18] S.S. Han, H.M. Lee, Carbon 42 (2004) 2169.
[19] A. Ansón, M.A. Callejas, A.M. Benito, W.K. Maser, M.T. Izquierdo, B. Rubio, J. Jagiello, M. Thommes, J.B. Parra, M.T. Martínez, Carbon 42 (2004) 1237.
[20] S.M. Lee, Y.H. Lee, Appl. Phys. Lett. 76 (2000) 2877.
[21] S.M. Lee, K.H. An, Y.H. Lee, G. Seifert, T. Frauenheim, J. Am. Chem. Soc. 123 (2001) 5059.
[22] Q. Wang, J.K. Johnson, J. Phys. Chem. B 103 (1999) 4809.
[23] M. Rzepka, P. Lamp, M.A. Casa-Lillo, J. Phys. Chem. B 102 (1998) 10894.
[24] F. Darkrim, D. Levesque, J. Phys. Chem. B 104 (2000) 6773.
[25] Y. Miyauchi, S. Chiashi, Y. Murakami, Y. Hayashida, S. Maruyama, Chem. Phys. Lett. 387 (2004) 198.
[26] M.J. Frisch et al., GAUSSIAN 03, Revision A.1, Gaussian, Inc., Pittsburgh, PA, 2003.
[27] L.G. Bulusheva, A.V. Okotrub, D.A. Romanov, D. Tomanek, J. Phys. Chem. A 102 (1998) 975.
[28] A. Rochefort, D.R. Salahub, P. Avouris, J. Phys. Chem. B 103 (1999) 641.
[29] Y.F. Zhang, J.Q. Li, M.X. Zhang, L.X. Zhou, Acta. Chim. Sinica. 60 (2002) 272.
[30] G.X. Jia, J.Q. Li, Y.F. Zhang, Acta. Chim. Sinica. 63 (2005) 97.
[31] J.Q. Li, Y.F. Zhang, M.X. Zhang, Chem. Phys. Lett. 364 (2002) 328.